EurJOC
European Journal of Organic Chemistry

Research Article
doi.org/10.1002/ejoc.202400847

Chemistry Europe
European Chemical Societies Publishing

www.eurjoc.org

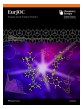

N-Arylphenothiazines and *N*,*N*-Diarylphenazines as Tailored Organophotoredox Catalysts for the Reductive Activation of Alkenes

Madeleine Giraud,[a] Mathis Robin Mitha,[a] Sven Klehenz,[a] and Hans-Achim Wagenknecht*[a]

A small library of *N*-arylphenothiazines, *N*-arylbenzo[*b*]phenothiazines and *N*,*N*-diarylphenazines has been synthesized as strongly reducing organophotocatalysts without the need for sacrificial reagents or electrochemistry. Their optoelectronic properties and their suitability as organophotoredox catalysts for the efficient activation of olefins was investigated using the addition of methanol to α-methylstyrene as a model reaction. The findings were supported by DFT calculations. Three photocatalysts were identified that allowed quantitative yields with 10 mol% catalyst loading and 20 h irradiation by a 365 nm LED. The catalyst loading was gradually reduced to 0.5 mol% and the irradiation time was reduced to only 20 min. These experiments revealed that *N*,*N*-di*iso*butyl-4′-(10*H*-phenothiazin-10-yl)-[1,1′-biphenyl]-4-amine is the most efficient photocatalyst among the *N*-arylphenothiazines. This chromophore combines high electron density introduced by the di*iso*butylamino phenyl group with high absorptivity at 365 nm caused by the phenylene bridge to the phenothiazine core. In an attempt to shift the excitation wavelength into the visible light range for selectivity and sustainability purposes (potential use of sunlight as a light source), *N*-arylbenzo[*b*]phenothiazines *N*,*N*-diarylphenazines were designed that exhibit a red-shifted and broad absorbance shoulder into the visible range, but only *N*,*N*-diarylphenazines allow photocatalysis and the one-electron activation of alkenes by visible light (450 nm LED).

Introduction

Over the last decade, photoredox catalysis has become a versatile and powerful synthesis method in modern organic chemistry. Light, preferably in the UV–A or visible range, allows activation barriers to be overcome using photoinduced electron transfer pathways that are inaccessible via the conventional thermal approach.[1] Photoredox catalysis expands the repertoire of synthetic methods and overcomes limits of thermally activated synthetic methods,[2] in particular for late-state functionalizations.[3] The majority of currently available photocatalytic methods use transition metal complexes, in particular with ruthenium and iridium, due to their photophysical properties and their (photo)chemical robustness.[4] However, the use of metal-free organic chromophores as photoredox catalysts in combination with light from energy-saving LEDs can significantly improve sustainability. In the initial phase of this research, eosin y,[5] rhodamine 6G,[6] mesityl-[7] and aminoacridinium,[8] naphthochromenones,[9] and 4,6dicyanobenzenes[10] were established for organophotoredox catalysis (Figure 1).[10] These organic chromophores offer a broad variety of different molecular scaffolds. Structural changes alter the physicochemical properties and allow tunability. Such synthetic tunability of organophotoredox catalysts is crucial to obtain the best-performing chromophore for specific reactions.[2b,11] Although originally invented for the metal-free atom transfer radical polymerisation (ATRP), *N*,*N*-diarylphenazines, *N*-arylphenothiazines and *N*-arylbenzo[*b*]phenothiazines also fulfil these requirements.[12] They show significant potential for organophotoredox catalysis because (1) they are synthetically well accessible, (2) their modular structure allows for the

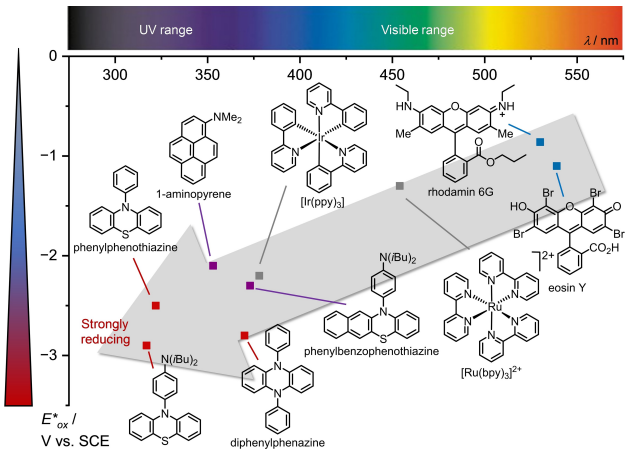

Figure 1. Absorption maxima λ_{max} in correlation to redox potentials in the excited state E^*_{ox} of $[Ir(ppy)_3]$, $[Ru(bpy)_3]^{2+}$ and selected organophotoredox catalysts to aim for strongly reducing photocatalysts.

[a] *M. Sc. M. Giraud, M. Sc. M. R. Mitha, M. Sc. S. Klehenz, Prof. Dr. H.-A. Wagenknecht*
Institute of Organic Chemistry, Karlsruhe Institute of Technology (KIT), Fritz-Haber-Weg 6, 76131 Karlsruhe, Germany
E-mail: Wagenknecht@kit.edu

Supporting information for this article is available on the WWW under https://doi.org/10.1002/ejoc.202400847

Research Article
doi.org/10.1002/ejoc.202400847

introduction of electron-donating or electron-withdrawing groups at the core and at the aryl group to tune the optoelectronic properties, (3) they are photochemically stable, and (4) they are strongly reducing photoredox catalysts.

The development of strongly reducing photoredox catalysts is an important task, enabling the photoactivation of less activated substrates, such as alkyl olefins and aryl chlorides, by single-electron reduction.[13] This requires advanced photoredox catalytic concepts such as (1) the consecutive photoelectron transfer concept (conPET) with perylene bisimides as photocatalysts,[14] (2) the sensitization-initiated electron transfer (SenI-ET), but both concepts are limited to aryl chlorides with electron-withdrawing groups and *N*-heterocycles,[15] (3) the use of the acridine radical with an excited state potential of −3.36 V vs SCE, pre-reduced by the sacrificial reagent $(i\text{Pr})_2\text{NEt}$,[16] (4) the electron-primed photoredox catalysis (epPRC),[17] and finally (5) the reductive electrophotocatalysis to obtain excited radical anions of dicyanoanthracene with a reduction potential of −3.2 V.[18] We aim for strongly reducing photocatalysis without the need for sacrificial reagents or electrochemistry. Here we present a small library of organophotoredox catalysts **1**–**17** comprised of *N*,*N*-diarylphenazines. *N*-arylphenothiazines, and *N*-arylbenzo[*b*]pheno-thiazines. By elucidating structure-activity relationships, the goal of this library is to derive tailored organophotocatalysts with strongly negative excited state reduction potentials to efficiently activate alkenes. Our[19] and others' recent results[20] show that these structure-activity relationships are crucial for efficient organophotoredox catalysis. Despite the strong reduction power of these chromophores, the goal is also to shift the excitation into the visible light range to gain selectivity and sustainability through the potential use of sunlight as a light source.

Results and Discussion

Synthesis of Organophotoredox Catalysts

The library of potential photoredox catalysts **X** contains the *N*,*N*-diphenylphenazine **5**, *N*-arylphenothiazines **6**–**15** and *N*-arylbenzo[*b*]phenothiazine **16**, **17** with structural variations by differently substituted aryl groups derived from the basic chromophores **1**,[21] **2**,[22] **3**,[23] and **4** (Figure 2).[24] They are typically excited in the UV–A range, ideally by a 365 nm LED. The reducing power of the organophotoredox catalysts is determined by the reduction potential in the excited state, $E_{ox}(\mathbf{X}^{\bullet+}/\mathbf{X}^{*})$, which is controlled by the *N*-aryl substituents. It therefore seemed to be reasonable to focus on electron-donating substituents at the aryl groups. Based on the unsubstituted **2**, this was first realized by methyl groups in **6**[25] and **7**,[26] by methoxy groups in **8**–**11**[23,27] and by the di*iso*butylamino group in **3**, using different substitution patterns. **12** and **13**[28] introduce the diphenylamino group as a replacement of the dialkylamino group. **14** carries two *tert*-butyl groups at the phenothiazine core to prevent stacking and to enhance the solubility in MeCN and MeOH. In **15**, the di*iso*butylaniline part and the phenothiazine core are separated by a phenylene bridge. The larger chromophore should increase its absorptivity at 365 nm. **16** and **17** contain extended π-systems, both with a naphthalene group instead of the simple phenyl group and a benzo[*b*]phenothiazine core to bathochromically shift the absorbance into the direction of the

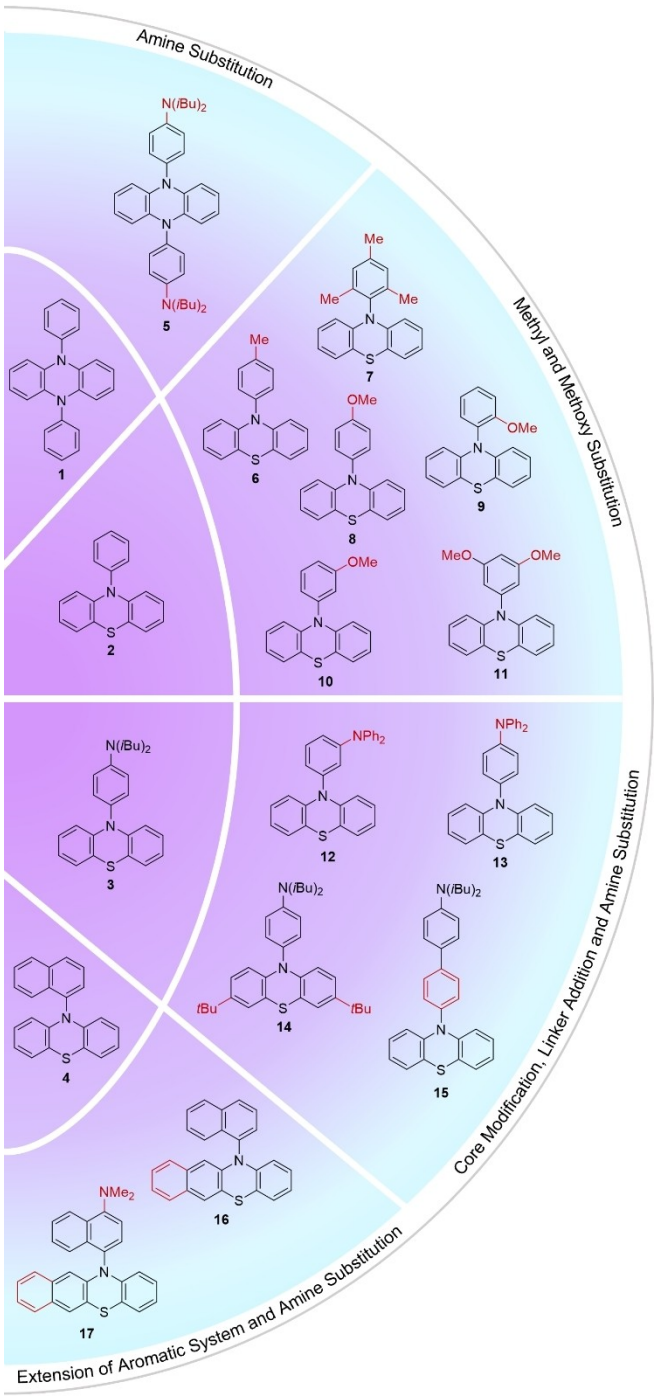

Figure 2. Library of organophotoredox catalysts **1**–**17** based on *N*,*N*-diphenylphenazine **1** and *N*-arylphenothiazines **2**–**4** as core structures. Amino substituents have been inserted based on **1**. **6**–**11** were modified with methyl and methoxy substituents based on **2**. Inspired by **3**, the amino substituents for **12** and **13** were changed. Based on **3**, the core of **14** was modified and **15** was extended by an phenylene linker. A benzene was fused with **3** to **16**, additionally modified by an amino substituent to **17**.

Research Article
doi.org/10.1002/ejoc.202400847

Chemistry Europe
European Chemical Societies Publishing

visible light range. *N,N*-diarylphenazines show such a red-shifted absorption with a tailing band into the visible light range already as the unmodified chromophore **1**. **5** is derived from and carries two di*iso*butylamino groups to gain stronger reduction potential in the excited state, similar to **3** for the *N*-arylphenothiazines.

The arylation of the core structures phenothiazine (**18**), benzo[*b*]phenothazine (**19**) and phenazine (**20**) at the nitrogen was performed by Buchwald-Hartwig aminations (Figure 3).[29] According to the general procedure arylbromide, NaO^{t}Bu, $Pd_2(dba)_3$ and PCy_3 are dissolved in dry toluene and heated at 120 °C (for all details see the Supporting Information).[30]

Spectroscopic and Electrochemical Characterization

N-arylphenothiazines, based on **2**, generally possess absorption maxima in the UV–A range around 320 nm (Figure 4 and Table 1). The tailing of this absorption band is typically used for excitation by the 365 nm LED. This general absorption feature is not significantly altered by any of the electron-donating groups in the chromophores **6–15**[23] (Figures S23–S28). That shows that simple substituents at the phenyl group do not significantly influence the optical properties of the *N*-arylphenothiazines. Only the extinction coefficients of **12** and **13** are relatively high (approximately 24,500 $M^{-1}cm^{-1}$) due to the additional *N*-phenyl groups that enlarge these chromophores. The chromophore of **15** was extended in a different way, by a phenylene bridge. As a result, its extinction coefficient is significantly increased to 33,300 $M^{-1}cm^{-1}$ at 324 nm. The higher extinction of **15** should allow lower catalyst loading which is advantageous for photocatalysis and sustainability (vide infra). The third alternative structural approach to enlarge the chromophore size is to fuse the phenothiazine core with benzene. Accordingly, the absorption maximum of the resulting *N*-arylbenzo[*b*]phenothiazine **16** is red-shifted to 350 nm and shows a broad shoulder due to the π-extended phenothiazine core with a higher extinction at 365 nm, too, similarly to **15**. Unexpectedly, such red-shifted absorption is not observed for the dimethylamino-substituted **17** (λ_{abs} = 325 nm) but there is still a red-shifted absorbance shoulder. In principle, this allows excitation by a 405 nm LED at the border of the visible light range.

The fourth type of extended chromophores is realized in the *N,N*-diarylphenazines **1** and **5** that have broad absorption maxima at 370 nm and 375 nm, respectively, with a slight tail up to about 475 nm (Figure 4). This allows their excitation in the visible light range, even with blue light (450 nm LED), although their extinction there is rather small (ε = 100 $M^{-1}s^{-1}$). Unexpectedly, the introduction of the two di*iso*butylamino groups in **5** lowered the exctinction at 365 nm significantly.

For the evaluation of the *N*-arylphenothiazines **2–4**, **6–15**, *N*-arylbenzo[*b*]phenothiazines **16–17** and the *N,N*-diarylphena-

Table 1. UV/Vis absorption maxima λ_{abs} (>300 nm) with extinction coefficients ε_{max} and $\varepsilon_{365\,nm}$, and fluorescence maxima λ_{em} of **1–17** in MeCN.

X	λ_{abs}/nm	λ_{em}/nm	ε_{max}/L mol^{-1} cm^{-1}	ε_{365nm}/L mol^{-1} cm^{-1}
1[21]	370	467	6,000	5,900
				100[a]
2[22,23]	320	443	3,400	500
3[23]	317	449	8,100	1,000
4[24]	316	373	5,000	1,100
5	375	476	2,900	2,700
				100[a]
6[25]	322	447	4,600	800
7[26]	328	444	4,800	1,200
8[27a]	322	448	3,900	700
9[27a]	317	441	3,800	500
10[27b]	316	444	3,500	500
11[23]	319	444	4,400	700
12	300	444	24,700	600
13[28]	303	444	24,300	300
14.	319	407	5,300	900
15	324	445	33,300	3,200
16	350	453	3,800	3,600
				1,300[b]
17	325	442	11,300	5,500
				1,600[b]

[a] ε_{450nm}. [b] ε_{405nm}.

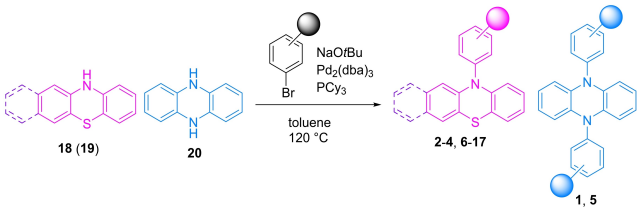

Figure 3. General procedure for the phenylation of the core structures phenothiazine (**18**), benzo[*b*]phenothazine (**19.**) and phenazine (**20**) at the nitrogen by Buchwald-Hartwig aminations to the organophotoredox catalysts **1–17**.[30]

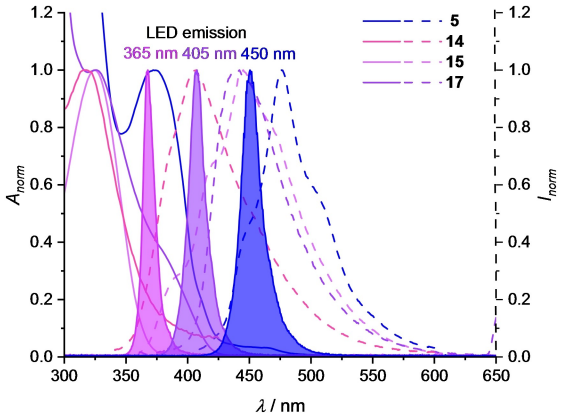

Figure 4. Normalized UV/Vis absorption and emission of the representative chromophores **5, 14, 15** and **17**, together with the emission of the 365 nm, 405 nm and 450 nm LEDs applied for the photocatalytic experiments.

Research Article
doi.org/10.1002/ejoc.202400847

zines **1**, **5** as organophotoredox catalysts, cyclic voltammetry (CV) was performed (Table 2). The reduction potential of the photocatalyst **X** in the excited state, E_1*(**X**$^{\bullet+}$/**X***) is the most critical value for the photocatalytic activity and calculated from the reduction potential E_1(**X**$^{\bullet+}$/**X**) derived from CV and E_{00} derived from UV/Vis absorption and fluorescence (Table 2). The initial electron transfer in the photocatalytic cycle is tuned by the *N*-aryl substituent(s), whereas the oxidation potential for the second electron transfer, E_1(**X**$^{\bullet+}$/**X**), closing the cycle, is controlled by the phenothiazine or phenazine core. For the *N*-arylphenothiazines, the weak electron-donating effect of the methyl groups in **6** and **7** do not significantly alter the excited state potential, E_1* is found at values of −2.5 V, similarly to **2**. The stronger methoxy groups in **8**–**11** shift the potential E_1* to −2.5 V−−2.7 V, but not as strongly as the di*iso*butylamino group in **3** and **14**, increasing the critical E_1* potentials to the remarkable value of −2.9 V. Although the diphenylamino groups in **12** and **13** combine both inductive and mesomeric electron-donating effects there are slightly weaker electron-donating substituents in comparison to the di*iso*butylamino groups, resulting in E_1* potentials in the range of −2.7−−2.8 V. The extension of the π-conjugated chromophore by the phenylene bridge in **15** reduces the E_1* potential slightly from −2.9 V−−2.7 V although this chromophore bears the strongly electron-donating di*iso*butylamino group. The extended benzo[*b*]phenothiazine core is an unsuccessful type of redox tuning because the E_1* potentials of **16** and **17** are significantly decreased to −2.0 V and −2.3 V. respectively.

Table 2. Reduction pote.ntials E_1(**X**$^{\bullet+}$/**X**), E_1(**X**$^{\bullet+}$/**X**) in the groundstate, E_{00} and E_{1*}(**X**$^{\bullet+}$/**X**) in the excited state of *N*-arylphenothiazines **2**–**4** and **6**–**15**, *N*-arylbenzo[*b*]-phenothiazine **16** and **17**, and *N*,*N*-diarylphenazine **1** and **5** (determined by cyclic voltammetry against Fc/Fc$^+$, converted to SCE[31]).

X	E_1(X$^{\bullet+}$/X)/V	E_2(X^{2+}/X$^{\bullet+}$)/V	E_{00}/eV	E_{1*}(X$^{\bullet+}$/X*)/V
1	0.13	0.94	2.96	−2.8
2[23]	0.75	1.50[a]	3.20	−2.5
3[23]	0.45	0.92	3.35	−2.9
4	0.71	–	3.55	−2.8
5[b]	0.03	0.75.	2.93	−2.9
6	0.65	1.49	3.16	−2.5
7	0.63	1.55	3.11	−2.5
8	0.66	1.47	3.27	−2.7
9	0.71	1.40	3.28	−2.5
10	0.69	1.45	3.25	−2.6
11	0.73	1.36	3.16	−2.4
12[c]	0.66	0.96.	3.50	−2.8
13[d]	0.65	0.97	3.30	−2.7
14	0.45	0.91	3.39	−2.9
15[e]	0.63	0.83	3.36	−2.7
16	1.03	–	3.03	−2.0
17	0.73	0.94	3.04	−2.3

[a] Irreversible potential. [b] Additional potential at E = 1.23 V. [c] Additional irreversible potential at E = 1.33 V. [d] Additional irreversible potential at E = 1.42 V. [e] Additional irreversible potential at E = 1.43 V.

The *N*,*N*-diarylphenazine 1 shows as an unmodified chromophore already the strongly negative E_1* potential of −2.8 V. Unexpectedly, the di*iso*butylamino group in **5** (vs. **1**) does not exhibit an as strongly electron-donating effect on the E_1* potential (−2.9 V) as the *N*-arylphenothiazines **3** and **14** (vs. **2**). This shows that structure-activity relationships cannot be simply transferred from one chromophore type to the other, even if they are quite similar.

Photoredox Catalytic Addition of Methanol

As a model reaction for the evaluation of the photocatalytic capabilities of **1**–**17**, the nucleophilic Markovnikov-type addition of alcohols, here simply methanol, to olefins, here α-methylstyrene (**21**), is used. After excitation of the photoredox catalyst **X** (**X** = **1**–**17**) an electron is transferred onto the substrate **21** (Figure 5). The resulting substrate radical anion **21**$^{\bullet-}$ is immediately protonated and the neutral radical **21H**$^{\bullet}$ is formed. The second electron transfer to **X**$^{\bullet+}$ converts the substrate into the electrophilic cation **21H**$^+$ and reacts with the nucleophile, here methanol, to the final addition product **22**. The mesomeric stabilization of both the radical **21H**$^{\bullet}$ and the cation **21H**$^+$ explains the Markovnikov regioselectivity of this addition.

The standard conditions include 10 mol% of the photocatalyst **X**, the use of a 365 nm LED, and an irradiation time of 20 h. The yields (Table 3) were determined by ^{1}H NMR spectroscopy.[23] The potential of **21** lies between that of α-phenylstyrene, E_{red}(S/S$^{\bullet-}$) = −2.3 V, and that of styrene, E_{red}(S/S$^{\bullet-}$) = −2.6 V.[32] After excitation of the photoredox catalyst an electron can only be transferred onto the substrate **21** if the oxidation potential in the excited state is sufficiently high. This threshold becomes evident by the photocatalytic experiments: Nearly all members of our chromophore library photocatalyze the conversion of the substrate **21** into the product **22**, only the *N*-arylbenzo[*b*]phenothiazines **16** and **17** with an excited state potential of only −2.0 V and −2.3 V do not show any significant photocatalytic activity, neither at 365 nm nor at 405 nm. Our *N*-arylbenzo[*b*]phenothiazines are therefore not capable of alkene activation by one-electron reduction, not even, if they are

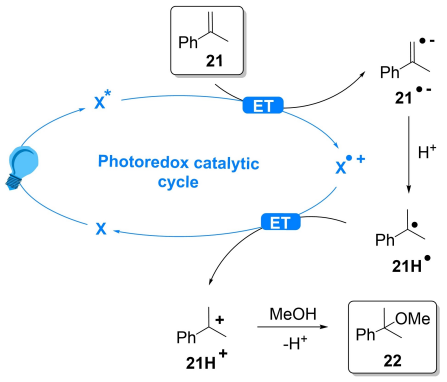

Figure 5. Proposed mechanism for the photoredox catalyzed addition of MeOH to α-methylstyrene (**21**) into p.roduct **22** with Markovnikov orientation, ET = electron transfer, irr.adiation by 365 nm, 405 nm or 450 nm LED.[23]

Table 3. Yields for the conversion of substrate **21** (170 μmol in 1 mL MeOH) into product **22** by using photocatalysts **1–17**. Irradiation by 365 nm, 405 nm or 450 nm LEDs for 20 h at 35 °C with vigorous stirring.[23]

X	λ/nm	mol%	t/h	yield/%
1	365	10	20	quant.
		1	3	quant.
		0.5	3	99
		0.5	1	99
		0.5	0.33	88
	450	10	20	quant.
		1	3	47
		0.5	3	37
2	365	10	20	54
3	365	10	20	quant.
		1	3	72
		0.5	3	46
4	365	10	20	24
5	365	10	20	quant.
		1	3	quant.
		0.5	3	99
		0.5	1	90
		0.5	0.33	79
	450	10	20	quant.
		1	3	31
		0.5	3	6
6	365	10	20	66
7	365	10	20	54
8	365	10	20	72
9	365	1.0	20	48
10	365	10	20	57
11	365	10	20	73
12	365	10	20	17
13	365	10	20	39
14	365	10	20	quant.
		1	3	51
		0.5.	3	46
15	365	10	20	quant.
		1	3	98
		0.5	3	98
		0.5	1	54
16	365	10	20	7
	405	10	20	–[a]
17	365	10	20	2
	405	10	20	–[a]

[a] Traces only.

modified with the strongly donating dimethylamino group (**17**). This type of structural tuning does not work for this chromophore type. The redox tuning by different electron-donating groups of the *N*-arylphenothiazines **6–11** works and gives yields between 48%−73%. The catalysts **6** and **7** with the weakly electron-donating methyl groups show comparable yields to **9** and **10** with the strongly electron-donating methoxy groups in ortho- and meta-position. The para-position of the methoxy substituent in **8** further increases the yield compared to **9** and **10**. The two methoxy groups make photocatalyst **11** as efficient as **8**. Unexpectedly, with **12** and **13** only low to moderate yields of 17% and 39% were achieved, although they bear the electron-donating diphenylamino groups. This is not only due to their relatively low E_1* potentials but can also be explained by the irreversible E_1 potentials found in the cyclic voltammograms of **12** and **13** (Figures S45 and S46) that indicate their photocatalytic instability. Their unspecific photodegradation during irradiation is one of the reasons why **21** is poorly converted. Quantitative yields were only achieved with the chromophores **1**, **3**, **5**, **14**, and **15**. This is a prerequisite for advanced photocatalytic experiments. The catalyst loading was gradually reduced to 1 mol% and further to 0.5 mol% using reduced irradiation times of 3 h, 1 h and finally only 20 min. These experiments revealed that **15** is the most efficient catalyst among the *N*-arylphenothiazines, as only with this photocatalyst excellent yields (98%) were still possible under these challenging conditions (0.5 mol%, 3 h) when irradiated at 365 nm. Even after irradiation for only 1 h a yield of 54% was still obtained. The other *N*-arylphenothiazines **1**, **3** and **14** bearing only the di*iso*butylamino group, could not give as high yields under the same demanding conditions. **15** is an example of successful structural tuning because it combines the strong reduction potential in the excited state E_1*(**15**$^{\bullet+}$/**15***) = −2.7 V influenced by the di*iso*butylamino group with the high extinction coefficient of $\varepsilon_{365nm} = 3{,}200\ M^{-1}cm^{-1}$ caused by the phenylene group. The phenazines **1** and **5** as the third type of chromophore in this library also show remarkable photocatalytic activity, because comparably high yields (88% and 79%) of product **22** were obtained under the advanced photocatalytic conditions with only 0.5 mol% chromophore and 20 min irradiation at 365 nm. More remarkably, both also allow the quantitative conversion of substrate **21** with visible light (450 nm LED), but only with high catalyst loadings of 10 mol% and 20 h of irradiation. At this wavelength, the more demanding photocatalytic conditions (0.5 mol%, 3 h) significantly reduce the yield of product **22**–37% (with **1**) and to only 6% (with **5**). The photocatalyst tuning of *N*,*N*-diphenylphenazines by the two di*iso*butylamino groups fails because the photocatalytic activity of **5** is not better than that of **1**. This stands in contrast to the *N*-arylphenothiazines and the positive effect of electron-donating substituents on their photocatalytic activity, as discussed above. Additional experiments were conducted with **5** and **15** in MeCN, using only stoichiometric amounts of MeOH. However, this significantly reduced the yield of **22**, especially at low catalyst concentrations of 1 mol% and only 3 h of irradiation (Table S2). The instability of the photocatalysts is not enhanced in those experiments.

Research Article
doi.org/10.1002/ejoc.202400847

DFT Calculations of Conformation, HOMO and LUMO

In order to gain a better understanding of the photoreactivity, DFT calculations of the chromophores **1**–**17** and their respective radical cations were carried out at the B3-LYP[34]/def2-TZVP[35] level of theory with DFT–D4 dispersion correction,[36] using TURBOMOLE[37] (version 7.7.1). As frequency analysis did not show any imaginary frequencies, it was confirmed that only energy minimum structures were obtained. For all calculated molecules, the quasi-equatorial intra-configuration was revealed to be the minimum energy structure. This was expected due to the electron-donating properties of the substituents on the nitrogen.[38]

In the ground state, both *N*-arylphenothiazines **2**–**4**, **6**–**15** and *N*-arylbenzo[*b*]phenothiazines **16**, **17** show a curved "butterfly" conformation along the S–N axis, which has already been reported for other phenothiazine derivatives.[38,39] The corresponding radical cations, on the other hand, have a more planar geometry, as already described by us and by Müller *et al.* for **3**.[19,38] The *N*,*N*-diarylphenazines **1**, **5** show a planar geometry in both states.

We focused on the calculations of the frontier orbitals of the *N*-arylphenothiazines and *N*-arylbenzo[*b*]phenothiazines. The calculated HOMOs and LUMOs of **13**, **14**, **15** and **17** are visualized representatively (Figure 6, for the HOMOs and LUMOs of the other compounds, see Figures S51–S67). The HOMO is localized on the phenothiazine core. The LUMO is localized on the aryl substituent and is critical for photocatalytic activity because the photoinduced electron transfer from here initiates the photoredox catalytic cycle. Its energy is influenced by the electron-donating property of the substituent(s) on the aryl group. This correlation can be seen for the *N*-arylphenothiazines **2**, **3**, and **6**–**14** with different photocatalytic activity, as discussed above. However, the photocatalytic activity of **12** and **13** with the diphenylamino group is lower than that of **14** with the di*iso*butylamino group. In addition to the possible reasons mentioned above, this could be explained by the calculated LUMO of **13** showing a significant delocalization not only on the phenyl ring of the *N*-phenylphenothiazine but also on the two phenyl rings at the amino group. Obviously, this delocalization has the positive effect that the molar UV extinction rises. On the down side, however, it reduces the electron-donating effect on the initial electron transfer from the photoexcited electron in the former LUMO and makes **13** a less efficient photocatalyst than **14**. This explains why the structural tuning by the diphenylamino groups failed. The most efficient photocatalyst in the *N*-arylphenothiazine series is **15**. The calculated LUMO shows electron density not only on the phenylene bridge but also delocalization over the di*iso*butylaminophenyl group, similar to **14**. This rationalizes the significantly enlarged extinction coefficient of **15** ($\varepsilon_{365\,nm} = 3{,}200\ M^{-1}\,cm^{-1}$) in comparison to **14** ($\varepsilon_{365\,nm} = 900\ M^{-1}\,cm^{-1}$) allowing nearly quantitative conversions with lower photocatalyst loadings of 0.5 mol% and shortened irradiation time of 3 h.

With **14**, the same photocatalytic conditions result in a significantly reduced yield of only 46%. As mentioned already above, **15** combines high electron density introduced by the

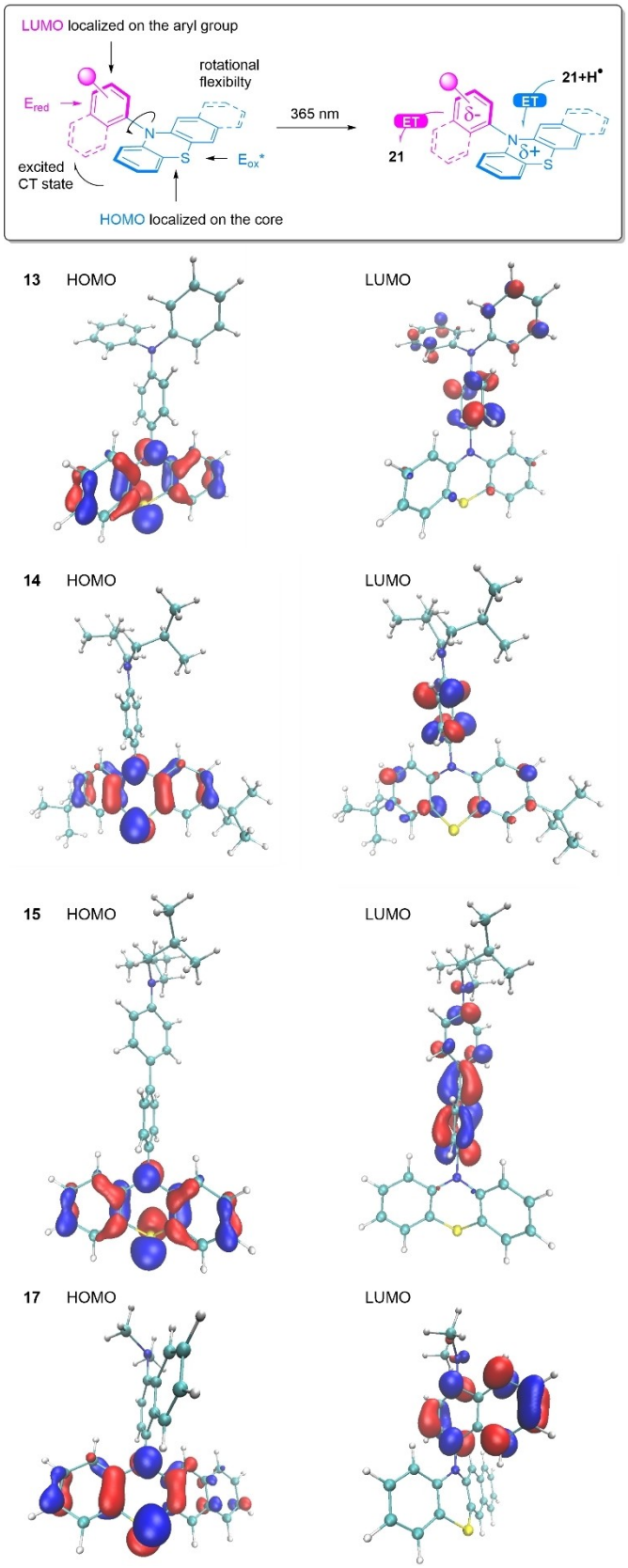

Figure 6. Principal photochemistry of *N*-phenylphenothiazines and calculated HOMOs and LUMOs of **13**, **14**, **15** and **17** (for the others see Supporting Information). All structures and frontier orbitals were visualized using VMD[33] version 1.9.3.

Research Article
doi.org/10.1002/ejoc.202400847

di*iso*butylamino group with high absorptivity at 365 nm caused by the phenylene group. For the benzo[*b*]phenothiazines **16** and **17** the larger π-conjugated chromophore core should enable photocatalysis at 405 nm, the threshold to visible light. These experiments, however, fail and only traces of product **22** could be detected, if at all. The calculated conformation of the **17** shows a significant curvature in the benzo[*b*]phenothiazine core of this chromophore. As a result, the delocalization of the electron-density is not equal throughout the whole benzo[*b*]phenothiazine core, with only a very low electron density of the HOMO on the benzo-fused ring. This explains why **17** principally behaves like a phenothiazine in the photocatalysis and only shows conversion by irradiation at 365 nm. The product yield after irradiation at 365 nm is only 7% (**16**) and 2% (**17**) due to their too low redox potentials E_1* as discussed above. Overall, the tuning of photocatalytic activation of alkenes by the *N*-arylbenzo[*b*]phenothiazines was not successful.

Despite the described differences between the calculated LUMOs and HOMOs, there is an obvious correlation between the calculated LUMO energies of **1**–**17** and the photocatalytic yields obtained under identical conditions (10 mol% **X**, 20 h irradiation at 365 nm, Figure 7). Higher LUMO energies (less negative values), result in greater photocatalytic yields for product **22**. This clearly reflects the influence of the LUMO energy by the electron-donating property of the substituent(s) on the aryl group. Since the initial photoinduced electron transfer originates from this molecular orbital it is crucial for the outcome of the photocatalysis. With the photocatalysts **1**, **3**, **5**, **14** and **15** quantitative yields were obtained for the conversion of substrate **21** under standard conditions. Only for **15**, the calculated LUMO energy does not fit well enough with the obtained high yield in photocatalysis. In this case, not only the electron-donating di*iso*butylamino substituent but also the enlarged chromophore must be considered that promotes the photocatalytic activity by the enhanced absorptivity.

For the activation of aryl chlorides by using **3** as photocatalyst we recently evidenced a consecutive two-photon process.[19] It was spectroscopically shown that the phenothiazine radical cation $\mathbf{3}^{\bullet+}$ (formed after the initial photoinduced electron transfer onto the substrate **21**) is excited a second time and undergoes a photoinduced shift of the positive charge to the *N*-aryl substituent (Figure 8 top). To support this hypothesis also for **5**, **14** and **15**, spectroelectrochemistry was applied to measure the absorbance of their radical cations $\mathbf{5}^{\bullet+}$, $\mathbf{14}^{\bullet+}$ and $\mathbf{15}^{\bullet+}$ (Figure 8 bottom). The absorbance of the radical cations $\mathbf{14}^{\bullet+}$ and $\mathbf{15}^{\bullet+}$ overlaps well with the emission of the 365 nm LED. We therefore assume that a consecutive two-photon photocatalytic mechanism, similarly to **3**, takes place during irradiation of these two chromophores. In comparison, the radical cation $\mathbf{5}^{\bullet+}$ shows a smaller overlap with the emission of the 365 nm LED than $\mathbf{14}^{\bullet+}$, $\mathbf{15}^{\bullet+}$ which makes a consecutive two-photon mechanism at 365 nm less likely. Catalyst **5** can also be excited with visible light at 450 nm, where a consecutive two-photon mechanism is enabled by the strong overlap of the LED emission with the absorption of $\mathbf{5}^{\bullet+}$. This explains why a quantitative conversion of **21**–**22** was achieved after 20 h of irradiation by the 450 nm LED although the extinction of **5** at 450 nm LED is much smaller than at 365 nm.

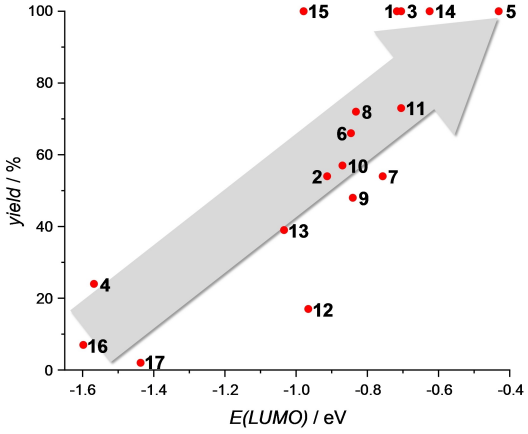

Figure 7. Correlation between LUMO energies of **1**–**17** with the photocatalytic yields of product **22** obtained under identical experimental conditions: Irradiation for 20 h by the 365 nm LEDs at 35 °C with vigorous stirring and a photocatalyst loading of 10 mol%.

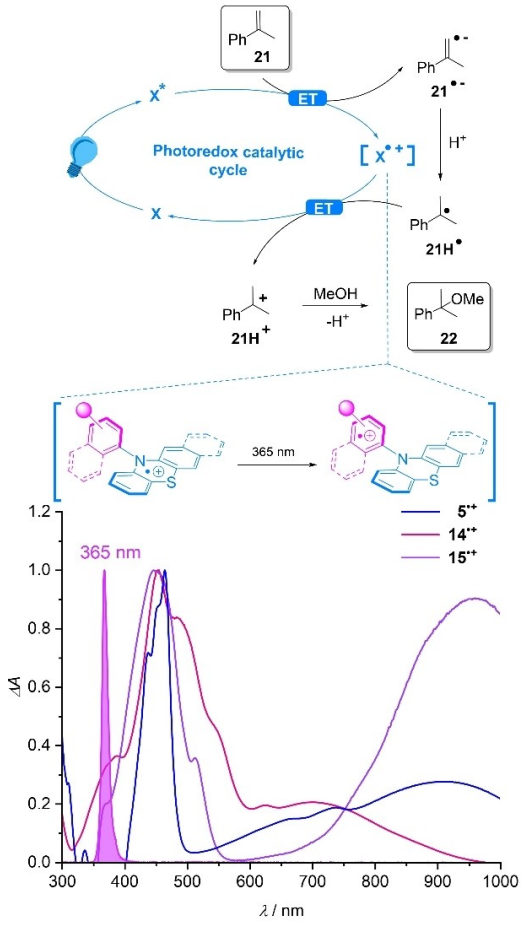

Figure 8. Top: Proposed photocatalytic mechanism with charge shift in the photocatalyst induced by a second photon in the cycle. Bottom: Spectroelectrochemistry with **5**, **14** and **15**: Absorbance of the radical cations $\mathbf{5}^{\bullet+}$, $\mathbf{14}^{\bullet+}$ and $\mathbf{15}^{\bullet+}$ in comparison to the normalized emission of the 365 nm LED.

Conclusions

In conclusion, we presented a small library of *N*-arylphenothiazines, *N*-arylbenzo[*b*]phenothiazines and *N,N*-diarylphenazines **1**–**17** to aim for strongly reducing photocatalysts without the need for sacrificial reagents or electrochemistry. The goal of this library was to derive tailored organophotocatalysts to efficiently activate alkenes. We compared the opto-electronic properties and the suitability as organophotoredox catalysts using the Markovnikov-type addition of methanol to the styrene **21** as a model reaction. These findings were corroborated by DFT calculations and spectroelectrochemistry. The novel chromophores **5**, **14** and **15** allowed quantitative yields with 10 mol% catalyst loading and 20 h irradiation. Here, the catalyst loading was gradually reduced to 1 mol% and further to 0.5 mol% using reduced irradiation times of 3 h, 1 h and finally only 20 min. These experiments revealed that **15** is the most efficient catalyst among the *N*-arylphenothiazines. This chromophore is the result of successful structural tuning and combines high electron density introduced by the di*iso*butylamino group with high absorptivity at 365 nm caused by the phenylene group. In a further tuning attempt, the excitation should be shifted into the visible light range to gain selectivity and sustainability by the potential use of sunlight as a light source. To enlarge the chromophore size a benzene was fused with the phenothiazine core. The resulting *N*-arylbenzo[*b*]phenothiazines **16** and **17** are red-shifted and show a broad absorbance shoulder into the visible range. However, *N*-arylbenzo[*b*]phenothiazines are not capable of alkene activation by one-electron reduction, even not, if they are modified with the strongly donating dimethylamino group ion **17**. Structural tuning by strongly electron-donating groups does not work for this chromophore type. The *N,N*-diarylphenazine **1** and **5** are larger chromophores than the *N*-arylphenothiazines and show a red-shifted absorption with a slight tail up to about 475 nm allowing their excitation in the visible light range (450 nm LED). Unexpectedly, the di*iso*butylamino group in **5** does not exhibit a strong electron-donating effect which shows that structure.-activity relationships cannot be simply transferred from chromophore type to the other, not even, if they are quite similar.

Acknowledgements

Financial support by the Deutsche Forschungsgemeinschaft (grant Wa 1386/23-1) and the KIT is gratefully acknowledged. We thank Simon Heckmeier for the initial synthesis of the two arylbenzo[*b*]phenothiazines. Open Access funding enabled and organized by Projekt DEAL.

Conflict of Interests

The authors declare no conflict of interest.

Data Availability Statement

The data that support the findings of this study are available in the supplementary material of this article.

Keywords: Photocatalysis · Photochemistry · UV/Vis absorption · Fluorescence · Electrochemistry

[1] a) F. Glaser, C. Kerzig, O. S. Wenger, *Angew. Chem. Int. Ed.* **2020**, *59*, 10266–10284; b) T. H. Rehm, *ChemPhotoChem* **2019**, *3*, 1–21; c) F. Strieth-Kalthoff, M. J. James, M. Teders, L. Pitzer, F. Glorius, *Chem. Soc. Rev.* **2018**, *47*, 7190–7202; d) D. M. Arias-Rotondo, J. K. McCusker, *Chem. Soc. Rev.* **2016**, *45*, 5803–5820.
[2] a) S. K. Pagire, T. Föll, O. Reiser, *Acc. Chem. Res.* **2020**, *53*, 782–791; b) N. A. Romero, D. A. Nicewicz, *Chem. Rev.* **2016**, *116*, 10075–10166; c) L. Marzo, S. K. Paigre, O. Reiser, B. König, *Angew. Chem. Int. Ed.* **2018**, *57*, 10034–10072; d) G. E. M. Crisenza, D. Mazzarella, P. Melchiorre, *J. Am. Chem. Soc.* **2020**, *142*, 5461–5476; e) L. Capaldo, D. Ravelli, *Eur. J. Org. Chem.* **2020**, 2783–2806; f) D. Ravelli, M. Fagnoni, A. Albini, *Chem. Soc. Rev.* **2013**, *42*, 97–113; g) T. Rigotti, J. Alemán, *Chem. Commun.* **2020**, *56*, 11169–11190.
[3] a) P. Bellotti, H. M. Huang, T. Faber, F. Glorius, *Chem. Rev.* **2023**, *123*, 4237–4352; b) R. Cannalire, S. Pelliccia, L. Sancineto, E. Novellino, G. C. Tron, M. Giustiniano, *Chem. Soc. Rev.* **2021**, *50*, 766–897.
[4] a) M. H. Shaw, J. Twilton, D. W. C. MacMillan, *J. Org. Chem.* **2016**, *81*, 6898–6926; b) D. Staveness, I. Bosque, C. R. J. Stephenson, *Acc. Chem. Res.* **2016**, *49*, 2295–2306.
[5] D. P. Hari, B. König, *Chem. Commun.* **2014**, *50*, 6688–6699.
[6] I. Ghosh, L. Marzo, A. Das, R. Shaikh, B. König, *Acc. Chem. Res.* **2016**, *49*, 1566–1577.
[7] K. A. Margrey, D. A. Nicewicz, *Acc. Chem. Res.* **2016**, *49*, 1997–2006.
[8] B. Zilate, C. Fischer, C. Sparr, *Chem. Commun.* **2020**, *56*, 1767–1775.
[9] J. Mateos, F. Rigodanza, A. Vega-Penaloza, A. Sartorel, M. Natali, T. Bortolato, G. Pelosi, X. Companyó, M. Bonchio, L. Dell'Amico, *Angew. Chem. Int. Ed.* **2020**, *59*, 1303–1312.
[10] E. Speckmeier, T. G. Fischer, K. Zeitler, *J. Am. Chem. Soc.* **2018**, *140*, 15353–15365.
[11] a) A. Vega-Penaloza, J. Mateos, X. Comanyó, M. Escudero-Casao, L. Dell'Amico, *Angew. Chem. Int. Ed.* **2020**, *60*, 1082–1097; b) T. Bortolato, S. Cuadros, G. Simionato, L. Dell'Amico, *Chem. Commun.* **2022**, *58*, 1263–1283.
[12] a) J. C. Theriot, C.-H. Lim, H. Yang, M. D. Ryan, C. B. Musgrave, G. M. Miyake, *Science* **2016**, *352*, 1082–1085; b) N. J. Treat, H. Sprafke, J. W. Kamer, P. G. Clark, B. E. Barton, J. R. d. Alaniz, B. P. Fors, C. J. Hawker, *J. Am. Chem. Soc.* **2014**, *136*, 16096–16101.
[13] X. Li, Y.-L. Tu, X.-Y. Chen, *Eur. J. Org. Chem.* **2024**, *27*, e202301060.
[14] I. Ghosh, T. Ghosh, J. I. Bardagi, B. König, *Science* **2014**, *346*, 725–728.
[15] I. Ghosh, R. S. Shaikh, B. König, *Angew. Chem. Int. Ed.* **2017**, *56*, 8544–8549.
[16] I. A. MacKenzie, L. Wang, N. P. R. Onuska, O. F. Williams, K. Begam, A. M. Moran, B. D. Dunietz, D. A. Nicewicz, *Nature* **2020**, *580*, 76–82.
[17] N. G. W. Cowper, C. P. Chernowsky, O. P. Williams, Z. K. Wickens, *J. Am. Chem. Soc.* **2020**, *142*, 2093–2099.
[18] H. Kim, H. Kim, T. H. Lambert, S. Lin, *J. Am. Chem. Soc.* **2020**, *142*, 2087–2092.
[19] F. Weick, N. Hagmeyer, M. Giraud, B. Dietzek-Ivansic, H.-A. W. agenknecht, *Chem. Eur. J.* **2023**, *29*, e202302347.
[20] N. Sugihara, Y. Nishimoto, Y. Osakada, M. Fujitsuka, M. Abe, M. Yasuda, *Angew. Chem. Int. Ed.* **2024**, *63*, e202401117.
[21] H. Wieland, *Liebigs Ann. Chem.* **1911**, *381*, 200–216.
[22] H. Gilman, P. R. V. Ess, D. A. Shirley, *J. Am. Chem. Soc.* **1944**, *66*, 1214–1216.
[23] F. Speck, D. Rombach, H.-A. Wagenknecht, *Beilstein J. Org. Chem.* **2019**, *15*, 52–59.
[24] T. Liu, Y.-G. Wei, Y.-Q. Yuan, Q.-X. Guo, *Chin. J. Chem.* **2005**, *23*, 1430–1436.
[25] H. Gilman, R. D. Nelson, J. F. Champaigne, Jr., *J. Am. Chem. Soc.* **1952**, *74*, 4205–4207.
[26] T. Gessner, W. Kowalsky, C. Schildknecht, *World Intellectual Property Organization*, Patent WO2006056416A1, Basf Aktiengesellschaft, Germany, **2006**.

[27] a) E. R. Biehl, H. S. Chiou, S. Kennard, J. Keepers, P. Reeves, *J. Heterocycl. Chem.* **1975**, *12*, 397–399; b) D. Clarke, B. C. Gilbert, P. Hanson, *J. Chem. Soc.-Perkin Trans.* **1976**, *2*, 114–124.
[28] P. Kathirgamanathan, Patent GB2513013B, Power OLEDS Limited, United Kingdom **2014**.
[29] a) J. Louie, J. F. Hartwig, *Tetrahedron Lett.* **1995**, *36*, 3609–3612; b) A. S. Guram, S. L. Buchwald, *J. Am. Chem. Soc.* **1994**, *116*, 7901–7902; c) F. Paul, J. Patt, J. F. Hartwig, *J. Am. Chem. Soc.* **1994**, *116*, 5969–5970.
[30] Y.-J. Cheng, S.-Y. Yu, S.-C. Lin, J. T. Lin, L.-Y. Chen, D.-S. Hsiu, Y. S. Wen, M. M. Lee, S.-S. Sun, *J. Mater. Chem. C* **2016**, *4*, 9499–9508.
[31] V. V. Pavlishchuk, A. W. Addison, *Inorg. Chim. Acta* **2000**, *298*, 97–102.
[32] R. S. Ruoff, K. M. Kadish, P. Boulas, E. C. M. Chen, *J. Phys. Chem.* **1995**, *99*, 8843–8850.
[33] W. Humphrey, A. Dalke, K. Schulten, *J. Mol. Graphics* **1996**, *14*, 33–38.
[34] a) A. D. Becke, *J. Chem. Phys.* **1993**, *98*, 5648–5652; b) C. Lee, W. Yang, R. G. Parr, *Phys. Rev. B* **1988**, *37*, 785–789; c) A. D. Becke, *Phys. Rev. A* **1988**, *38*, 3098.
[35] F. Weigend, R. Ahlrichs, *Phys. Chem. Chem. Phys.* **2005**, *7*, 3297–3305.
[36] E. Caldeweyher, C. Bannwarth, S. Grimme, *J. Chem. Phys.* **2017**, *147*, 034112.
[37] F. Furche, R. Ahlrichs, C. Hättig, W. Klopper, M. Sierka, F. Weigend, *Wiley Interdiscip. Rev.: Comput. Mol. Sci.* **2014**, *4*, 91–100.
[38] L. Mayer, L. May, T. J. Müller, *Org. Chem. Front.* **2020**, *7*, 1206–1217.
[39] J. McDowell, *Acta Cristallogr. B* **1976**, *32*, 5–10.

Manuscript received: July 26, 2024
Revised manuscript received: August 28, 2024
Accepted manuscript online: August 28, 2024